EurJIC European Journal of Inorganic Chemistry

MICROREVIEW

DOI: 10.1002/ejic.201100894

Lanthanide Complexes as Paramagnetic Probes for ^{19}F Magnetic Resonance

Peter Harvey,[a] Ilya Kuprov,*[b] and David Parker*[a]

Keywords: Fluorine / MRI / Relaxation / Lanthanides / Paramagnetism / NMR spectroscopy

The physicochemical basis of probe design for ^{19}F MRS and MRI applications is reviewed. Complexes that give a single major resonance in solution are described, in which the Ln^{3+} ion is about 6 Å from the ^{19}F label. Sensitivity improvements of 15-fold are reported in both imaging and spectroscopy based on longitudinal relaxation enhancement. The pseudocontact shift allows an amplification of chemical shift non-equivalence in responsive ^{19}F probes, e.g. for monitoring pH in the range between 5 and 8.

Introduction

The fluorine nucleus is an attractive probe for chemical and biological magnetic resonance studies.[1] The high receptivity (^{19}F, I = 1/2, 100% abundance) and similar Larmor frequency to the ^{1}H nucleus (188 MHz at 4.7 T) allow the use of tunable dual probes based on common instrumentation for spectroscopy or imaging studies. Despite the absence of a background signal, the acquisition of sufficient signal intensity in a reasonable time period remains the limiting feature of ^{19}F MR studies. This is most evident for imaging applications where the total spin concentration of the fluorinated probe or material needs to be typically in the 10–50 mM range. The use of hyperpolarised ^{19}F-MRI reduces this limit considerably, notwithstanding the restriction of very short acquisition times.[2] Thus, most imaging applications have been based on probes derived from perfluorocarbon emulsions, or fluorine-labelled polymers and dendrimers.[3–7]

[a] Department of Chemistry, Durham University,
South Road, Durham, DH1 3LE, U.K
Fax: 44-191-334-2051
E-mail: david.parker@durham.ac.uk
[b] Oxford e-Research Centre,
7 Keble Road, Oxford, OX1 3QG, U.K
E-mail: ilya.kuprov@oerc.ox.ac.uk

Peter Harvey graduated with a Masters in Chemistry in 2009 at Durham University; his studies included research into spin-crossover complexes of iron(II). He is currently a Ph.D. candidate working with Professor Parker and his research relates to the design and synthesis of responsive paramagnetic lanthanide complexes for use in ^{19}F magnetic resonance.

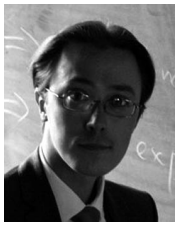

Ilya Kuprov is an EPSRC Advanced Fellow at the Oxford e-Research Centre. He specializes in large-scale spin dynamics simulations, relaxation theory and spin chemistry.

David Parker has been a Professor of Chemistry at Durham University since 1992. He has been a member of successive COST Chemistry Actions since 1995, working in collaboration with groups in Turin, Alessandria, Coimbra and Tubingen. His research interests in coordination chemistry embrace design, mechanistic and stereochemical aspects, aligned with the definition of function in emissive and magnetic resonance probes. He is a Fellow of the Royal Society (2002) and received the RSC Ludwig Mond Award in Inorganic Chemistry in 2011.

Aside from improving the targeting of a fluorinated probe or conjugate, sensitivity in the MR studies may also be enhanced by increasing the rate of longitudinal relaxation of the ^{19}F nucleus. This may be achieved by introduction of a proximate paramagnetic centre, such as a d- or f-block metal ion or complex. With a series of lanthanide complexes, the reduction in T_1 from values of the order of 1 s to about 10 ms allows more rapid data acquisition per unit time, provided that the concomitant decrease in T_2 does not impair detection sensitivity too much.[8,9] Indeed, the merits and demerits of this approach need to be assessed thoughtfully. For example, if there is an intermolecular interaction between the fluorinated probe and the paramagnetic metal centre, then the encounter probability is inherently low and relaxation enhancement effects are only modest. The encounter contact time can be increased by making use of ion-pairing[10] or non-covalent binding.[11–12] A more versatile and controllable approach is to make the interaction intramolecular, by positioning the ^{19}F nucleus at a fixed distance from the paramagnetic ion, preferably in the range 4.5 and 7.5 Å.[8] The steepness of the distance dependence (r^{-6}) of the electron–nuclear dipolar relaxation rate interaction defines this working range: too close, and line-broadening is severe; too distant, and the longitudinal relaxation rate increase is normally less than a factor of ten and the sensitivity gain is much reduced.

An additional aspect of ^{19}F NMR studies is the broader chemical shift range in comparison with ^{1}H magnetic resonance spectroscopy. This feature has promoted the development of ^{19}F MR to follow changes in the composition of a fluorinated compound, e.g. metabolism studies in vivo with a fluorinated drug.[13,14] In addition, it has encouraged the creation of fluorinated probes, in which the observed chemical shift reports on the local environment.[1] Some examples of such "responsive probes" have appeared in which the chemical shift reports an irreversible transformation of the fluorinated probe, for example, by bond cleavage catalysed by an endogenous enzyme.[15] Of greater intrinsic interest are responsive ^{19}F MR probes involving a reversible process, induced by modulation of the local chemical environment, e.g. reporting pH, pM or pX variation. Chemical shift probes are much more useful, as those based on signal intensity modulation retain a dependence on probe concentration. Examples of some diamagnetic ^{19}F chemical shift probes have been devised,[1] but their insensitivity and modest $\Delta\delta_F$ values (typically $\delta \leq 2$ ppm) limit their utility. However, when the ^{19}F nucleus is close to a lanthanide ion within the same molecule, the dipolar (pseudocontact) shift can amplify the chemical shift non-equivalence.[8,9,16] Amongst the Ln^{3+} ions, this shift effect does not apply for gadolinium; the magnetic susceptibility tensor of the Gd^{3+} ion is almost isotropic due to the lack of orbital degeneracy in its ground state.

Theoretical Background

The design principles for successful ^{19}F lanthanide MR probes are based on an appreciation of the theory defining the ability of each Ln^{3+} ion to cause nuclear relaxation and include a paramagnetic shift.

Pseudocontact Shift as a Response Amplification Mechanism

Conformational change is normally a low-energy process that does not produce large variations in the chemical shielding of either protons or fluorine. The biggest change found in practice (e.g. for a shift from an axial to an equatorial position with respect to an aromatic ring) is about 5 ppm for both ^{1}H and ^{19}F NMR spectroscopy.[17] More often, changes in δ_F are <1 ppm, corresponding to a frequency difference of <120 Hz at a field of 3 T, which can be difficult to detect by using MRI. An amplification mechanism is therefore required to make conformational changes more easily detected by nuclear shielding measurements.

A very convenient MRI response amplification mechanism is provided by the pseudocontact shift (PCS) – the rotationally invariant component of the dipolar interaction between the nuclei and the Curie magnetisation induced on the unpaired electrons by the applied magnetic field.[18] Because the electron magnetisation supplements the applied magnetic field, the interaction experimentally manifests itself as additional chemical shielding of the nuclei. The derivation of PCS[19] is beyond the scope of this review, but the resulting expressions feature strong directional dependence[18] [Equations (1) and (2)].

$$\delta(r,\theta,\varphi) = \frac{1}{12\pi r^3}\left[\chi_{ax}\left(3\cos^2\theta - 1\right) + \frac{3}{2}\chi_{rh}\sin^2\theta\cos 2\varphi\right] \quad (1)$$

$$\delta(x,y,z) = \frac{1}{12\pi r^3}\left[\chi_{ax}\frac{2z^2 - x^2 - y^2}{r^2} + \frac{3}{2}\chi_{rh}\frac{x^2 - y^2}{r^2}\right] \quad (2)$$

where $\{r,\theta,\phi\}$ are spherical coordinates of the nucleus, χ_{ax} is the axiality of the electron magnetic susceptibility tensor, χ_{rh} is its rhombicity and the coordinate system is aligned to the eigensystem of the susceptibility tensor with the electron (assumed to be a point particle) located at the origin.

A typical distribution of pseudocontact shift (for a given probe nucleus it may be viewed as a 3D scalar field) is schematically illustrated in Figure 1. At a distance of 4 to 5 Å from the lanthanide ion, the chemical shift difference associated with a conformational change can in practice be around 50 ppm,[19] making it very easy to detect by MRI. This may be seen directly in Figure 1 – if an aromatic ring is labelled with a CF_3 group, conformational changes can potentially shift the fluorine nucleus from an area with a strong positive PCS (red) to an area with a strong negative PCS (blue); such a change is easily detected. Certain lanthanide complexes possess Bleaney[18] coefficients of opposite sign (Table 1), and this can also lead to very different pseudocontact shifts for common resonances in a given com-

Table 1. Selected magnetic and relaxation properties of lanthanide(III) ions.

Lanthanide ion	Ground state term	μ_{eff}/μ_B[a]	μ_{eff}/μ_B (expt.)[b]	Electron relaxation time (aqua ion, 2.1 T) / 10^{-13} s[d]	$\langle S_Z \rangle$[f]	Rel. PCS strength[c,g]
Ce^{3+}	$^2F_{5/2}$	2.56	2.55	0.90	–0.97	–6.5
Pr^{3+}	$^3H_4$	3.62	3.47	0.57	–2.96	–11.4
Nd^{3+}	$^4I_{9/2}$	3.68	3.69	1.15	–4.45	–4.5
Pm^{3+}	$^5I_4$	2.68	2.41	unknown	–3.94	2.4
Sm^{3+}	$^6H_{5/2}$	1.55–1.65	1.58	0.45	0.22	–0.5
Eu^{3+}	$^7F_0$	3.40–3.51	3.4	0.09	7.57	4.0
Gd^{3+}	$^8S_{7/2}$	7.94	7.63	10^4–10^5[e]	31.5	0
Tb^{3+}	$^7F_6$	9.7	9.8	2.03	31.9	–87
Dy^{3+}	$^6H_{15/2}$	10.6	10.3	2.99	28.6	–100
Ho^{3+}	$^5I_8$	10.6	10.4	1.94	22.6	–39
Er^{3+}	$^4H_{15/2}$	9.6	9.4	2.38	15.4	32
Tm^{3+}	$^3H_6$	7.6	7.6	3.69	8.21	53
Yb^{3+}	$^2F_{7/2}$	4.5	4.3	1.37	2.59	22

[a] Ref.[24] [b] Refs.[9,25] [c] Ref.[18] [d] Ref.[26] [e] Ref.[27] [f] Ref.[28] [g] Refs.[18,29]

plex. The strong dependence of the PCS on the nuclear coordinates makes it possible to enhance the response of the contrast agent to environmental parameters (such as pH) by coupling those parameters to molecular conformation.

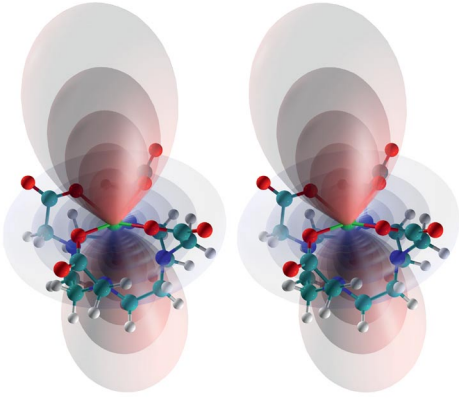

Figure 1. Schematic stereodrawing of the pseudocontact shift field around the archetypal [Ln·DOTA]$^-$ complex, with an axial magnetic susceptibility tensor (the main axis is directed vertically in the plane of the picture).

We have recently published a proof of principle pH measurement that takes advantage of this effect: a pH-induced conformational change in [HoL^1] (Scheme 1 below) is associated with a ^{19}F chemical shift change of 18 ppm when the pH changes from 6.0 to 9.0.[9,16] Because tumour tissue is often more acidic than healthy tissue (due to glycolysis-dominated metabolism),[20] this raises the possibility of detecting tumours that might not otherwise be visible in an MRI scan. A change of conformation can also, in principle, be coupled to other local parameters (redox potential, dielectric constant, pM, pX). Pseudocontact shift variation therefore can provide a very general means of tracking changes in a variety of chemical parameters by using magnetic resonance spectroscopy or chemical shift imaging.

Nuclear Spin Relaxation Due to Electron–Nuclear Interactions

Relaxation behaviour of open-shell systems is well researched,[21] and at high magnetic fields the relatively straightforward Bloch–Redfield–Wangsness theory[22] is applicable. For the paramagnetic lanthanide complexes in question, the diamagnetic NMR relaxation mechanisms (through internuclear dipolar interactions and chemical shielding anisotropy) are negligible, and the primary contribution comes from the rotational and conformational modulation of the electron–nuclear dipolar interaction [Equations (3) and (4)].[9]

$$R_1 = \frac{2}{15}\left(\frac{\mu_0}{4\pi}\right)^2 \frac{\gamma_N^2 \mu_{eff}^2}{r^6}\left[\frac{7\tau_{R+e}}{1+\omega_e^2\tau_{R+e}^2} + \frac{3\tau_{R+e}}{1+\omega_N^2\tau_{R+e}^2}\right] + \frac{2}{5}\left(\frac{\mu_0}{4\pi}\right)\frac{\omega_N^2 \mu_{eff}^4}{(3kT)^2 r^6}\frac{3\tau_R}{1+\omega_N^2\tau_R^2} \quad (3)$$

$$R_2 = \frac{1}{15}\left(\frac{\mu_0}{4\pi}\right)^2 \frac{\gamma_N^2 \mu_{eff}^2}{r^6}\left[4\tau_{R+e} + \frac{3\tau_{R+e}}{1+\omega_N^2\tau_{R+e}^2} + \frac{13\tau_{R+e}}{1+\omega_e^2\tau_{R+e}^2}\right] + \frac{1}{5}\left(\frac{\mu_0}{4\pi}\right)^2 \frac{\omega_N^2 \mu_{eff}^4}{(3kT)^2 r^6}\left[4\tau_R + \frac{3\tau_R}{1+\omega_N^2\tau_R^2}\right] \quad (4)$$

where μ_0 is vacuum permeability, γ_N is the magnetogyric ratio of the nucleus (in this case ^{19}F), r is the electron–nuclear distance, τ_R is the rotational correlation time (isotropic rotational diffusion assumed), ω_N is the nuclear Larmor frequency, T is the absolute temperature, k is the Boltzmann constant and the remaining symbols are defined as follows:

$$\mu_{eff}^2 = g_J^2 \mu_B^2 J(J+1), \quad \tau_{R+e} = \left(\tau_R^{-1} + T_{1e}^{-1}\right)^{-1}, \quad \omega_e = \left(\frac{g_J \mu_B}{\hbar}\right) B_0$$

in which g_J is the effective electron g-factor, μ_B is Bohr magneton, $J(J + 1)$ is the effective electron angular momentum

averaged over the thermally populated electronic energy levels and T_{1e} is the longitudinal relaxation time of the electron spin. The first term in each equation comes from the stochastic modulation of the electron–nuclear dipolar interaction by molecular rotation and random jumps of the electron magnetisation; the second term arises from the rotational modulation of the dipolar interaction of the nucleus with the average magnetic dipole moment induced in the electron shell by the applied magnetic field (so-called Curie relaxation[23]). Because f orbitals are localised on the metal, the point dipole approximation suffices in each case.

The dependence of the resulting relaxation rates on the effective magnetic moment and the electron–nuclear separation is illustrated in Figure 2. Both dipolar and Curie relaxation mechanisms have a reciprocal sixth power dependence on the electron–nuclear separation. Dipolar relaxation is quadratic in the effective magnetic moment of the electron (Table 1), and Curie relaxation asymptotically scales as μ_{eff}^4. From the experimental measurement perspective, the primary source of uncertainty is the temperature dependence of the relaxation rates – effective magnetic moment, electron relaxation rate and rotational correlation time all depend on temperature, which also occurs explicitly in the denominator of the Curie term. In experimental measurements, it is therefore essential to keep the temperature constant. Because longitudinal relaxation rates can be measured with very high precision, electron–nuclear distances, rotational correlation times and effective magnetic moments can be extracted.[9]

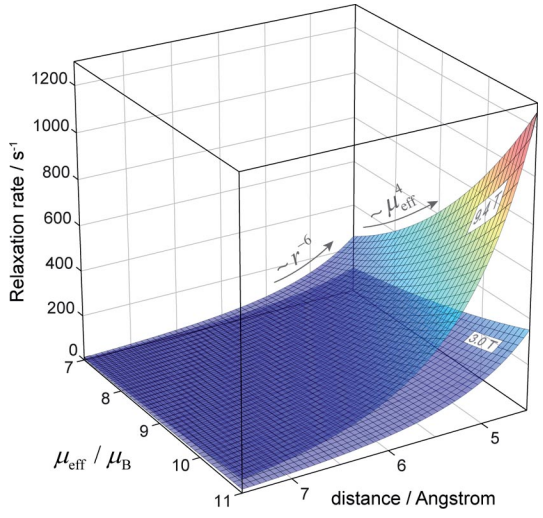

Figure 2. Longitudinal ^{19}F spin relaxation rate given by Equation (3) as a function of electron–nuclear separation (4.5 to 7.5 Å) and the effective magnetic moment of the electron at two different magnetic fields (corresponding to modern MRI instruments). The electron relaxation time, T_{1e}, was set to 0.2 ps, and the rotational correlation time, τ_r, is fixed at 250 ps, T = 298 K. The appearance of the transverse relaxation rate plots is nearly identical under these conditions.

As an example of this approach, ^{19}F longitudinal relaxation rates, R_1, were measured for [Ln·L^{1b}(H$_2$O)] at fields between 4.7 and 16.5 T. Using theoretical values of μ_{eff} (Table 1) and assuming that τ_e is 0.2 ps, a global fitting analysis of the five sets of data was used to give r = 6.3 Å and τ_r = 270 ps[9] (Figure 3). The steeper rise of R_1 with increasing field for the Dy and Ho complexes is ascribed to their higher μ_{eff} values and greater Curie contribution.

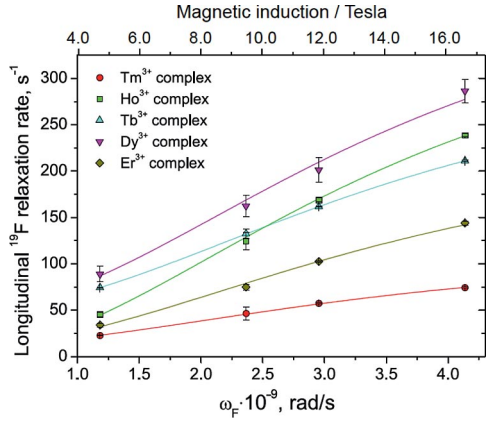

Figure 3. Variation of R_1 with magnetic field for [Ln·L^{1b}(H$_2$O)] (295 K, 1 mM complex). The coloured lines represent the global fit to Equation (3). Reprinted with permission from ref.[9] Copyright 1999 Wiley-VCH Verlag GmbH & Co. KGaA.

Structural Features of ^{19}F Lanthanide Probes: Speciation and Dynamic Exchange

Signal intensity is maximised if there is only one major ^{19}F resonance to observe. This means that the preferred ^{19}F labels are homotopic CF_3 groups, in a water-soluble complex where one major stereoisomer that is kinetically stable is present in solution.[9,30] Representative examples of such complexes are given in Scheme 1 and exemplify the importance of these issues.

The anionic complex, [Ln·L^5]$^-$, contains four trifluoroethyl groups, but ^{19}F NMR reveals the existence of a mixture of eight stereoisomeric species associated with the stereogenicity at each P centre (*RRRR*/*RRRS*/*RSRS*/*RRSS*) and the Δ/Λ helicity around the C_4 axis.[31] The neutral monoamide complexes, [Ln·L^2] and [Ln·L^3], differ considerably in behaviour.[9,30] The former exists as eight isomeric species, albeit with one preferred isomer, whose relative abundance changes slowly with time. In contrast, for the series Tb–Yb, the triphosphinate complex [Ln·L^3] gave rise to one dominant solution species (>87%) whose relative abundance was invariant with time. In the latter case, isomer exchange may be inhibited by the presence of the more bulky phosphinate groups. With each of these complexes, the CF_3 group maintains a constant distance (6 Å for Ln·L^3; 6.3 Å for [Ln·L^2]) from the Ln ion, owing to the rigidity associated with the aryl-amide coordination. This leads to R_1 values, (Table 2), of the order of 80 to 100 Hz for the Dy and Tb complexes, respectively (295 K, 4.7 T).

The homotopic perfluoro-*tert*-butyl group offers high spin density when incorporated into a lanthanide complex, notwithstanding its effect on water solubility. The lanthanide complexes [Ln·L^6] include a short helical oxyethylene chain to encourage water solubility.[32] The fluorinated

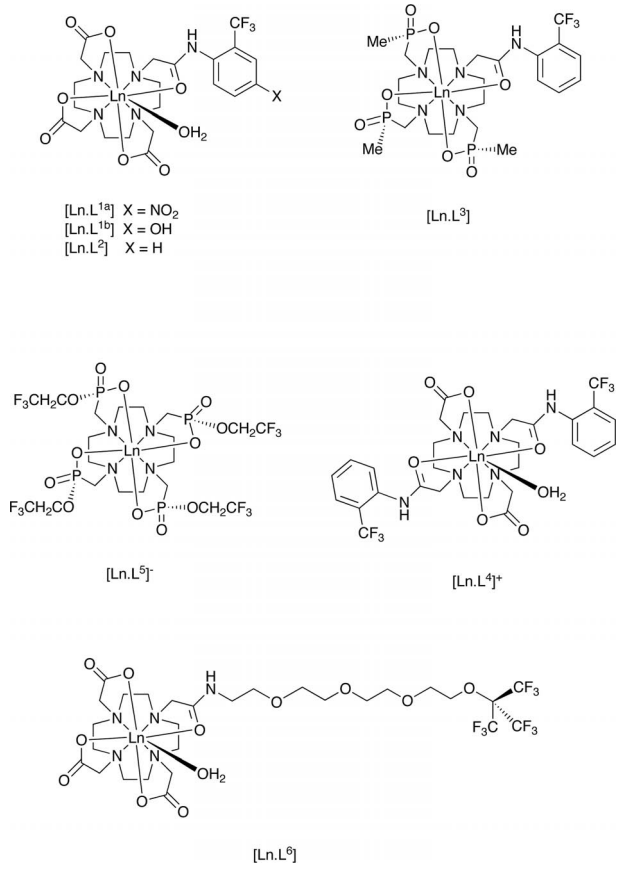

Scheme 1.

Table 2. ^{19}F NMR shift and relaxation data for [Ln·L^3][30] (295 K, pD 5.4, D_2O).

Ln	δ_F / ppm	R_1 / Hz		R_2 / Hz	
		4.7 T	9.4 T	4.7 T	9.4 T
Tb	–47.7	84	146	102	267
Dy	–63.6	104	185	135	251
Ho	–61.5	58	120	74	143
Er	–72.6	71	109	67	138
Tm	–89.5	46	63	60	84
Y	–61.2	1.2	2.5	3.8	5.5

moiety is more distant from the Ln^{3+} centre, and there is considerable chain flexibility. For the terbium complex, R_1 and R_2 values were 14 and 24 Hz, respectively (298 K, 11.7 T), which suggests that the perfluoroalkyl group is effectively about 10 Å distant from the Tb ion. Corresponding R_1/R_2 values for [Gd·L^6] are 238 and 588 Hz. The preeminence of the intramolecular electron–nuclear interaction in defining the R_1 and R_2 values means that these relaxation rates – provided that the mean separation r is not changing significantly and for a constant temperature – are usually not sensitive to changes in environment induced by ionic strength, pO_2 or other paramagnetic additives.

In the general case, chemical exchange processes can also lead to an increase in R_2, which causes line-broadening and reduced spectral sensitivity. Such processes may include either intramolecular conformational exchange e.g. through concerted "arm" rotation[33] or *E*/*Z* stereoisomer interconversion (e.g. around the amide bond in [Ln·L^1][16]), or intermolecular exchange between stereoisomeric or between "free" and "bound" species that are in equilibrium, associated with protonation, metal ion, anion or protein binding. Exchange broadening associated with prototropic exchange can be minimised by striving to work in the "slow-exchange regime" on the NMR timescale. This approach leads to a doubling (at least) of the observable signals, but means that the integrated ratio of the resonances directly reports their relative abundance and hence allows the equilibrium constant to be measured. Two examples illustrate this approach (Figures 4 and 5), and in each case, the shift in non-equivalence of the acid and base forms is amplified by the differing pseudocontact shifts.[16,9] The reversible binding of the arylsulfonamide nitrogen in the holmium complex (Figure 4) is associated with a pK_a of 5.71 in 0.1 M NaCl solution; in serum or urine, competitive hydrogen carbonate binding (fast exchange) shifts this equilibrium in favour of the "acid" form, and a pK_a of 6.92 was observed. The sulf-

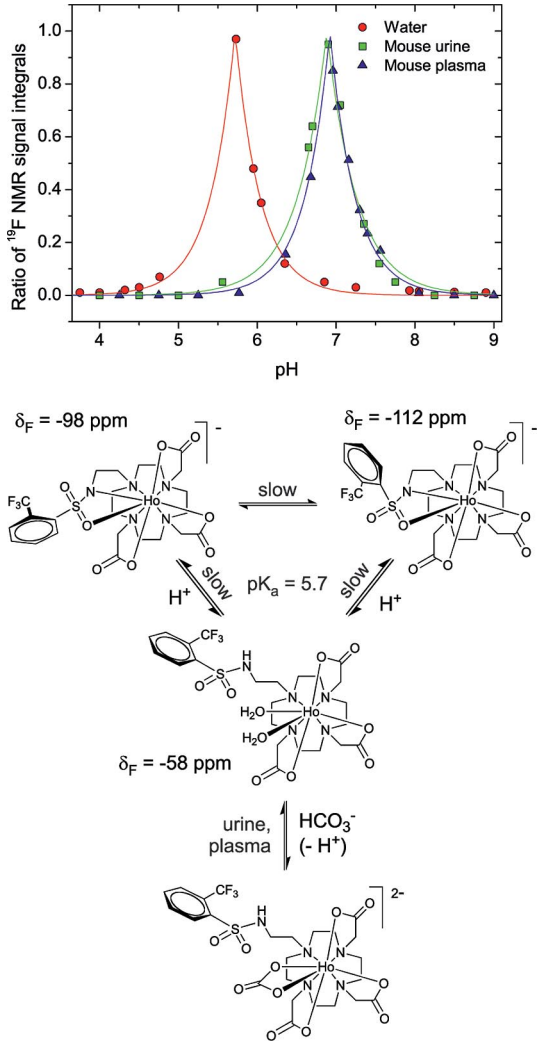

Figure 4. pH Dependence of the ^{19}F chemical shift for the holmium sulfonamide complex (295 K), showing the species present in solution either in water or in mouse urine or plasma.[16].

onamide bound and protonated species resonated 40 ppm apart in ^{19}F NMR spectrum, and the "basic" form was observed as two diastereoisomers (ratio 6:1), associated with an *R* or *S* configuration at sulfur (Figure 4); for the Tb analogue, this ratio was 9:1.

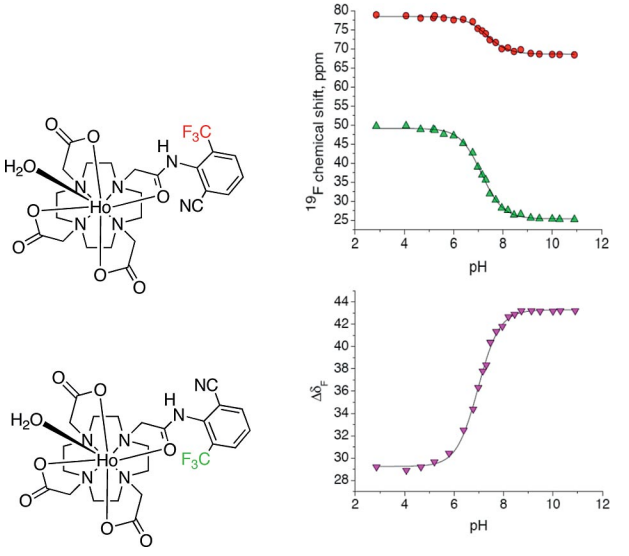

Figure 5. Variation of chemical shift with pH for the two isomeric holmium complexes, in which the protonation equilibrium involving the amide proton reveals a differing pH dependence for each isomer, allowing a $\Delta\delta_F$/pH plot to be used to define the pK_a (pK_a = 7.0, 295 K, 0.1 M NaCl). Reprinted with permission from ref.[9] Copyright 1999 Wiley-VCH Verlag GmbH & Co. KGaA.

A second example of a pH-responsive probe is provided by the *ortho*-cyano amide, shown in Figure 5. Amide deprotonation is associated with a pK_a of 7.0 (298 K, I = 0.1 M NaCl), and two major isomers were observed associated with restricted rotation about the aryl carbon–nitrogen bond. Each isomer exhibited not only a large shift nonequivalence but also differing pH-dependent shifts, such that their shift separation ($\Delta\delta_F \approx 14$ ppm) can be used to measure the solution pH.[9] These two approaches obviate the need for calibration of chemical shift, as the former example relies upon measuring a ratio of two signals and the latter measures a chemical shift separation.

Enhancing Sensitivity in MRS and MRI

The sensitivity gain by increasing longitudinal relaxation rates can be measured experimentally, by referencing the measured signal intensity to a diamagnetic analogue, e.g. the related yttrium(III) complex. For example, by using [Ln·L^3] in spectroscopy, sensitivity was improved by a factor of 5 to 15 – the Tb and Dy complexes prove most effective at 4.7 and 9.4 T (Table 3). This comparative analysis holds for complexes of this structural type, i.e. in which the CF_3 label is about 6 Å from the metal ion and where τ_r is of the order of 250 ps.[30] With the same complex, longitudinal and transverse relaxation rates at 7 T fall in the range 50–150 Hz and 70–200 Hz, respectively. Using a gradient echo imaging sequence, to achieve the maximum possible signal-to-noise ratio (SNR) per unit time in MRI, requires careful consideration of the sweep-width selected (SW), the repetition time (TR), the echo time (TE) and the flip angle.[34] As R_1 and R_2 are particularly sensitive to magnetic field [Equations (3) and (4)], the parameter set chosen is defined by the field used. The best results, which agree with theoretical enhancements, were observed for the dysprosium complex at 7 T, and a SNR of 211 (vs. 16 for the Y analogue) was achieved in <5 min with a 2 mM solution of the complex (Table 3). Such data is consistent with detection (allowing an SNR of 4 to define the limit) of 20 μM concentrations of the complex in tissue over a 15-min acquisition period. The sensitivity gain here is 13 times that of the diamagnetic analogue. A further sensitivity increase of a factor of two or three for [Dy·L^3] has been achieved by using a zero echo-time pulse sequence, working at 9.4 T.

Table 3. ^{19}F MRS[a] and MRI[b] experimental signal intensities (295 K, 2 mM complex, 15-min acquisition time for MRS, 4-min for MRI).[30,34]

Complex	4.7 T MRS	9.4 T MRS	7 T MRI
[Y·L^3]	1.0	1.0	1.0
[Tb·L^3]	14.4	15.2	8.4
[Dy·L^3]	12.5	14.9	13.2
[Ho·L^3]	6.6	9.3	10.9
[Er·L^3]	5.5	8.9	9.4
[Tm·L^3]	4.8	7.2	8.2

[a] A common line-broadening function was applied that was 50% of the observed linewidth, and the spectral acquisition time (per scan) was 3× T_1. [b] Phantom imaging data were acquired, by using experimental parameters (sweep width and repetition rate) defined by the theoretical maximum for each individual complex, according to their differing R_1 values,[34] with a 32-point matrix and a gradient echo imaging sequence. At a significantly higher imaging field, the Tb, Dy and Ho complexes became much less attractive, at least when $r \leq 6.5$ Å.

Prospects for Practicable Paramagnetic ^{19}F MR Probes

For in vivo MRSI/MRI applications, three key considerations are sensitivity of detection, the toxicity/tolerance and biodistribution profile of the probe and the feasibility of developing responsive probes for chemical shift imaging. In the case of sensitivity, improved probe design and detection systems should enhance prospects over the next decade. Over the field range 1.5 to 7 T, lanthanide-based ^{19}F probes offer sensitivity gains of between 15 to 20 times those of diamagnetic analogues. Permutation of the lanthanide ion may be required at higher fields, although Dy-based systems are likely to work best at lower fields. Variation of complex structure also allows control over R_1/R_2 values by changing the separation of the Ln/^{19}F label: for example, in [Dy·L^7] and [Dy·L^8] (Scheme 2), the CF_3 label is about 0.5 Å more distant and R_1 values decrease by 33% from 102 to 68 Hz (9.4 T, 295 K).

The clearance of these low MW probes occurs fairly quickly in vivo, through renal or biliary pathways determined by the charge and hydrophobicity of the complex.

This has been monitored by parallel ^{1}H MRI biodistribution studies with the Gd analogues of the same series of complexes:[35] this "dual imaging" approach should allow the co-registration of anatomical information and the idea has already been demonstrated by using directly injected fluorocarbon emulsions.[7] Higher MW conjugates in the range 5 to 15 kD will clear more slowly from the vasculature and offer longer imaging times. Examples include the polydisperse glycolchitosan conjugate, [Ln·L^{9}][35] containing an average of 12 CF_3 groups and the monodisperse PAMAM conjugate [Dy·L^{10}] (Scheme 2) with eight complexes linked to the periphery of the dendritic structure. Responsive probes may be based either on a low MW complex or be part of a conjugate. In each case, exchange broadening must be minimised and the desired change in chemical shift amplified by prior consideration of the location of the fluorine label with respect to the polar coordinates. Proof-of-principle studies with pH-responsible systems have been defined in vitro (vide supra) and now need to be translated into practice in vivo.

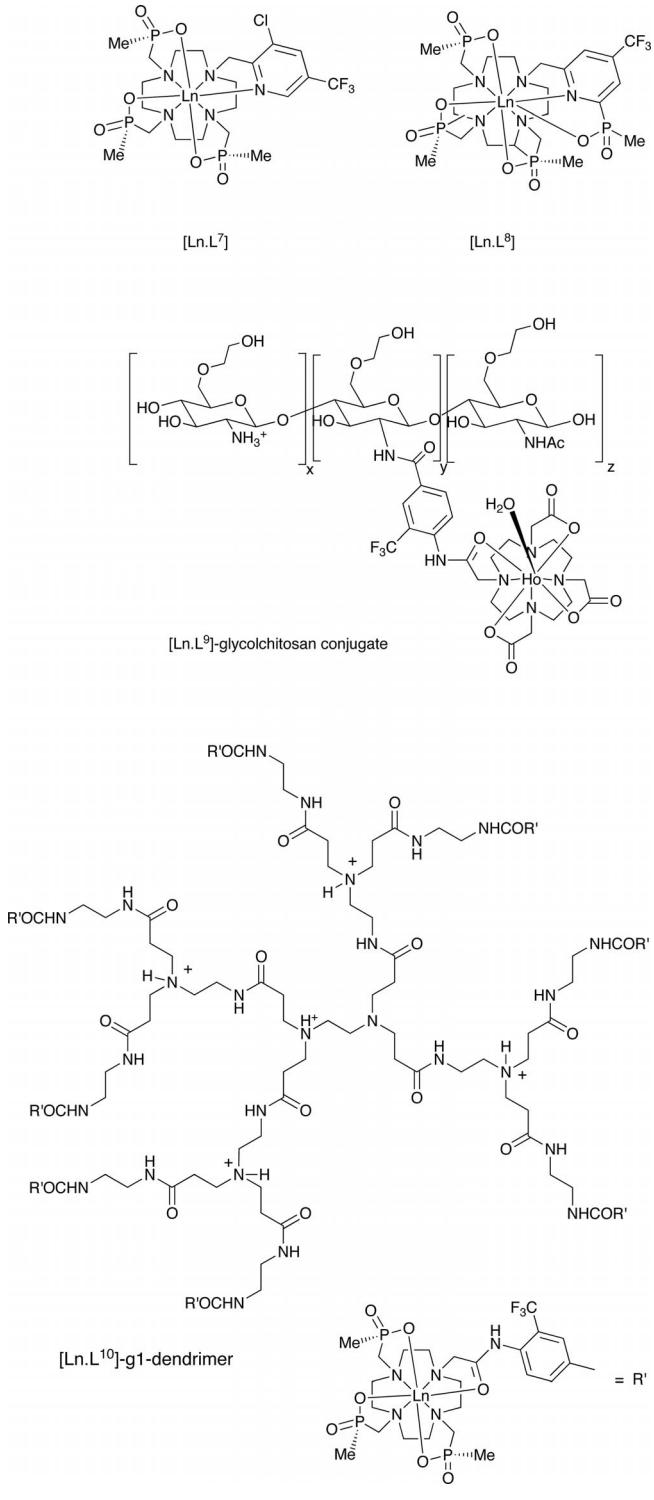

Scheme 2.

Acknowledgments

We thank EPSRC (EP/H003789/1), CRCUK and the ERC (FCC 266804) for support. This work was undertaken under the auspices of the COST D38 Action in collaboration with Prof. Mauro Botta (Alessandria). It is a pleasure to also thank Dr. Alan Kenwright (Durham), Profs. Andrew Blamire (Newcastle) and Cornelius Faber (Münster) for their assistance with this work.

[1] Y. Yu, V. D. Kodibagkar, W. Cui, R. P. Mason, *Curr. Med. Chem.* **2005**, *12*, 819.
[2] U. Bommerich, T. Trantzschel, S. Mulla-Osman, G. Buntkowsky, J. Bargon, J. Bernarding, *Phys. Chem. Chem. Phys.* **2010**, *12*, 10309.
[3] A. Neubauer, J. Myerson, S. D. Caruthers, F. D. Hockett, P. M. Winter, J. Chen, P. J. Gaffney, J. D. Roberson, G. M. Lanza, S. A. Wickline, *Magn. Reson. Med.* **2008**, *60*, 1066.
[4] M. Oishi, S. Sumitani, T. K. Bronich, A. V. Kabanov, M. D. Boska, Y. Nagasaki, *Chem. Lett.* **2009**, *38*, 128.
[5] Z. Huang, R. S. Sengar, A. Nigam, M.-C. Abadjian, D. M. Potter, D. B. Grotjahn, E. C. Wiener, *Invest. Radiol.* **2010**, *45*, 641.
[6] J. M. Criscione, B. L. Le, E. Stern, M. Brennan, C. Rahner, X. Papademetris, T. M. Fahmy, *Biomaterials* **2009**, *30*, 3946.
[7] B. Ebner, P. Behm, C. Jacoby, B. A. French, J. Schrader, U. Flogel, *Circ. Cardiovasc. Imaging* **2010**, *3*, 202.
[8] P. K. Senanayake, A. M. Kenwright, D. Parker, S. van der Hoorn, *Chem. Commun.* **2007**, 2923.
[9] K. H. Chalmers, E. De Luca, N. H. M. Hogg, A. M. Kenwright, I. Kuprov, D. Parker, M. Botta, J. I. Wilson, A. M. Blamire, *Chem. Eur. J.* **2010**, *16*, 134.
[10] S. Aime, A. Barge, J. I. Bruce, M. Botta, J. A. K. Howard, J. M. Moloney, D. Parker, A. S. de Sousa, M. Woods, *J. Am. Chem. Soc.* **1999**, *121*, 5762.
[11] E. Terreno, M. Botta, P. Boniforte, C. Bracco, L. Milane, B. Mandino, F. Uggeri, S. Aime, *Chem. Eur. J.* **2005**, *11*, 5531.
[12] E. Gianolio, R. Napditano, F. Fedeli, F. Arena, S. Aime, *Chem. Commun.* **2009**, 6044.
[13] L. D. Stegman, A. Rehemtulla, B. Beattie, A. Kievit, T. S. Lawrence, R. G. Blasberg, J. G. Tjuvajev, B. D. Ross, *Proc. Natl. Acad. Sci. USA* **1999**, *96*, 9821.
[14] W. E. Hull, R. E. Port, R. Herrmann, B. Britsch, W. Kunz, *Cancer Res.* **1988**, *48*, 1680.
[15] V. D. Kodibagkar, J. Yu, Y. Liu, H. P. Hetherington, R. P. Mason, *Magn. Reson. Imaging* **2006**, *24*, 459.
[16] A. M. Kenwright, I. Kuprov, E. De Luca, D. Parker, S. U. Pandya, P. K. Senanayake, D. G. Smith, *Chem. Commun.* **2008**, 2514.
[17] F. Khan, I. Kuprov, T. D. Craggs, P. J. Hore, S. E. Jackson, *J. Am. Chem. Soc.* **2006**, *128*, 10729.
[18] B. Bleaney, *J. Magn. Reson.* **1972**, *8*, 91.

[19] J. A. Peters, J. Huskens, D. J. Raber, *Prog. Nucl. Magn. Reson. Spectrosc.* **1996**, *28*, 283.
[20] K. M. Kennedy, M. W. Dewhirst, *Future Oncol.* **2010**, *6*, 127.
[21] J. Kowalewski, L. Nordenskiöld, N. Benetis, P.-O. Westlund, *Prog. Nucl. Magn. Reson. Spectrosc.* **1985**, *17*, 141.
[22] M. Goldman, *J. Magn. Reson.* **2001**, *149*, 160.
[23] M. Gueron, *J. Magn. Reson.* **1975**, *19*, 58.
[24] H. Gysling, M. Tsutsui, *Adv. Organomet. Chem.* **1970**, *9*, 361.
[25] I. Bertini, F. Capozzi, C. Luchinat, G. Nicastro, Z. Xia, *J. Phys. Chem.* **1993**, *97*, 6351; D. Gignoux, D. Schmitt, M. Zeguine, *J. Magn. Magn. Mater.* **1987**, *66*, 373; B. Chevalier, S. Tence, G. Andre, S. F. Matier, E. Gaudin, *J. Phys. Conf., Ser.* **2010**, *200*, 032012; J. Jensen, A. K. Mackintosh, *Rare Earth Magnetism*, **1991**, Oxford, Clarendon.
[26] B. M. Alsaadi, F. J. C. Rossotti, R. J. P. Williams, *J. Chem. Soc., Dalton Trans.* **1980**, 2151; see also: S. Aime, L. Barbero, M. Botta, G. Ermondi, *J. Chem. Soc., Dalton Trans.* **1992**, 225.
[27] I. Bertini, P. Turano, A. J. Vila, *Chem. Rev.* **1993**, *93*, 2833.
[28] A. A. Pinkerton, M. Rossier, S. Spiliadis, *J. Magn. Reson.* **1985**, *64*, 420.
[29] R. M. Golding, P. Pyykko, *Mol. Phys.* **1973**, *26*, 1389.
[30] K. H. Chalmers, M. Botta, D. Parker, *Dalton Trans.* **2011**, *40*, 904.
[31] W. D. Kim, G. E. Kiefer, J. Huskens, A. D. Sherry, *Inorg. Chem.* **1997**, *36*, 4128.
[32] Z.-X. Jiang, Y. Feng, Y. B. Yu, *Chem. Commun.* **2011**, *47*, 7233.
[33] R. S. Dickins, C. Crossland, J. A. K. Howard, D. Parker, H. Puschmann, *Chem. Rev.* **2002**, *102*, 1977.
[34] K. Chalmers, A. M. Kenwright, D. Parker, A. M. Blamire, *Magn. Reson. Med.* **2011**, *66*, 931.
[35] E. De Luca, Ph. D. Thesis, Durham University, **2010**; K. H. Chalmers, Ph. D. Thesis, Durham University, **2011**.

Received: August 25, 2011
Published Online: November 8, 2011

